Chemical Engineering & Technology Research Article 1

Irvan Dahlan[1,*]
Wan Hamizan Wan Mazlan[1]
Andi Mulkan[2]
Haider M. Zwain[3]
Siti Roshayu Hassan[4]
Hamidi Abdul Aziz[5]
Harahsheh Yazeed Ahmad Hasan[1]
Ivar Zekker[6]

Modeling of Batch Organic Dye Adsorption Using Modified Metal-Organic Framework-5

Modeling and simulation of batch adsorption of the organic dye methylene blue (MB) by modified metal-organic framework-5 (MOF-5) were investigated. The reported data on the adsorption of MB dye onto Wells-Dawson acids ($H_6P_2W_{18}O_{62}$)-immobilized MOF-5 were employed. The film-pore diffusion model was developed based on external mass transfer coefficient and pore diffusion coefficient that govern the mass transfer process in batch organic dye adsorption. Applying the estimated parameters, the MB adsorption by using modified MOF-5 was examined to evaluate the effects of MOF-5 modification, initial dye concentration, temperature, and the dosage of adsorbent. The adsorption capacity of modified MOF-5 ($H_6P_2W_{18}O_{62}$/MOF-5) was higher than pure MOF-5. Besides, a lower initial MB dye concentration, higher temperature, and lower adsorbent dosage resulted in higher MB dye adsorption capacity.

Keywords: Batch adsorption, Dye adsorption, Film-pore diffusion model, Metal-organic framework-5, Methylene blue

Received: January 19, 2022; *revised:* August 01, 2022; *accepted:* August 29, 2022

DOI: 10.1002/ceat.202200042

1 Introduction

Dyes, either natural dyes or synthetic dyes, have been exploited as coloring agents in a variety of industries, including textiles, cosmetics, paper, plastic, and leather [1, 2]. Over the last decade, the dye industry has grown at a tremendous pace, especially in China, India, and South Korea. China is the world's greatest producer and consumer of dyes, producing 70 % of global output and utilizing 55 % of global consumption. However, due to environmental protection and the pandemic condition, dye production and consumption have decreased in the last two years [3]. In term of market size, in 2020 the global dyes were valued at USD 32.9 billion and are predicted to rise at compound annual growth rate (CAGR) of 5.1 % from 2021 to 2028 [4].

According to a previously reported literature review by Gupta and Suhas [5], it was predicted that 700 000 to 1 000 000 tons of dyes are produced every year worldwide with more than 100 000 types of commercial dyes existing. At the same time, dye production and the textile dyeing processes use approximately 80 million tons and 90 million tons of water, respectively, each year. From these values and with the assumptions of 2 and 10 % of contaminated water generated from dye production and textile application, respectively, it was estimated that 11 million tons of water is being polluted every year [6].

Generally, dye wastewater has the following properties: great light and heat stability, oxidative agent resistance, and poor biodegradability. These organic compounds of dye contribute color to the aquatic environment after being released into water bodies, blocking sunlight transmission, and interfering the essential photosynthetic activities required for the balance of local ecosystem [7, 8]. Previously, the removal of diverse types of organic dyes has been done by using different methods and materials. For example, the removal of methylene blue (MB) dye has been studied by using a ZF-LDO/Co_3O_4 composite photoelectrocatalyst [9], ZnO and Ag framed nanocomposites (ZnO-Ag NPs) [10], and graphene oxide (GO)-containing

[1]Dr. Irvan Dahlan, Wan Hamizan Wan Mazlan, Harahsheh Yazeed Ahmad Hasan
chirvan@usm.my
School of Chemical Engineering, Universiti Sains Malaysia, Engineering Campus, 14300 Nibong Tebal, Pulau Pinang, Malaysia.
[2]Andi Mulkan
Mechanical Engineering Study Program, Faculty of Engineering, University of Iskandar Muda, Jalan Kampus Unida, Banda Aceh, 23234, Indonesia.
[3]Dr. Haider M. Zwain
College of Water Resources Engineering, Al-Qasim Green University, 51013 Babylon, Al-Qasim Province, Iraq.
[4]Dr. Siti Roshayu Hassan
Faculty of Bioengineering and Technology, Universiti Malaysia Kelantan, Jeli Campus, 17600 Jeli, Kelantan, Malaysia.
[5]Prof. Hamidi Abdul Aziz
School of Civil Engineering, Universiti Sains Malaysia, Engineering Campus, 14300 Nibong Tebal, Pulau Pinang, Malaysia.
[6]Dr. Ivar Zekker
Institute of Chemistry, University of Tartu, Ravila 14a, 50411 Tartu, Estonia.

hydrogels [11]. The removal of rhodamine B (RhB) dye has been investigated by means of photo-Fenton heterogeneous composite of FeNi@corncob-activated carbon [12], spindle-like cobalt oxide (Co_3O_4)-zinc oxide (ZnO) nanocomposites [13], and $CsPbBr_3$/$CsPb_2Br_3$@silica yolk-shell composite microspheres [14].

Photocatalytic degradation of methyl orange dye has been investigated by Rajput et al. [15] by using photocatalysis of TiO_2 nanomaterials. Besides, Si et al. [16] reported the preparation of Janus phenol-formaldehyde resin (PF) and periodic mesoporous organic silica (PMO) nanoparticles which have been effectively used to remove methyl orange dye. In addition, the β-cyclodextrin functionalized multilayer structured graphene membrane has been synthesized by a wet-chemical method and was successfully applied to remove methyl orange and (RhB) dyes [17].

Methylene blue (MB), a typical cationic dye, is a heterocyclic aromatic compound containing sulfur and is most commonly used in various fields including textiles, rubbers, varnishes, and medicals. This toxic organic dye may result in a variety of health issues such as cancer, hemolytic anemia, hypertension, skin staining, precordial pain, and injection site necrosis [18–20]. For these reasons, MB dye-containing wastewater is classified as hazardous waste and must be treated before being discharged into the water supply.

The removal of MB dye from wastewater poses a primary challenge. Many methods have been reviewed in the literature for the treatment of water and wastewater contaminated by organic dyes, especially MB dye, including adsorption [21], flocculation [22], advanced oxidation [23], plasma treatment [24], photocatalysis [25–28], and many others. From various treatment technologies existing, the adsorption technique using several types of adsorbents is still the most favorable method in the removal of these contaminants due to its efficiency, high adsorption capacity, and low operational cost [29]. Activated carbon (AC), from a variety of raw materials, is currently a hot topic among adsorbents. However, AC adsorption is still a costly technique and requires laborious regeneration procedures [21, 29].

Recently, metal-organic frameworks (MOFs) have attracted extensive research interest due to their novel properties. MOFs have shown great potentials in numerous applications [30, 31]. Due to their unique structures and properties, MOFs are highly suitable for high-performance supercapacitor electrode materials [32–34] and can improve the photochemical characteristics for degradation of RhB dye [35]. In addition, MOFs are a class of porous crystals that hold potential for many adsorption-based applications [36]. Because of their adsorptive characteristics and large surface area, MOFs could be used to remove organic dyes from industrial effluents.

MOFs are crystalline materials made up of nodes (metal ions or clusters) and linkers (organic ligands). The pore size, shape, and composition of MOFs can be controlled [19]. One of the most representative MOFs is MOF-5 [$Zn_4O(BDC)_3$]. It is a structure which is formed by groups of $(Zn_4O)_6^+$ clusters in octahedral subunits joined by 1,4-benzenedicarboxylic acid (BDC) linkers, to give an extended porous 3D framework [37]. Nonetheless, MOFs have been limited in their practical uses due to their poor processability and the fact that they are less thermodynamically stable than most inorganic microporous materials due to the presence of organic linkers.

Liu et al. [38] have modified MOF-5 by introducing Wells-Dawson acids ($H_6P_2W_{18}O_{62}$) for enhancing their reasonable properties towards selective adsorption capacity of MB dye. The results showed that the modified MOF-5 considerably increased the adsorption efficiency towards MB dye in aqueous solution. From previous studies, in comparison to their pristine MOF counterparts, several active species have been successfully introduced into MOFs to improve their specific properties, to add new functionalities and even synergetic features.

Apart from that, the important information related to equilibrium and kinetics of dye removal can be acquired from batch adsorption studies, which then can be used to advance research on continuing fixed-bed adsorption and to predict the adsorbent performance at industrial scale. Thus, the prediction of the rate of dye adsorption by the adsorbent particle is important for evaluating the adsorbent performance in the dye removal process. Besides, the process of adsorption by porous adsorbents also involves the external mass transfer, surface diffusion, intraparticle diffusion, and pore volume diffusion.

To gain further understanding of the features of dye and adsorbent for their surface contact, computational analysis is intended to be a complimentary tool. Recently, many theoretical and simulation approaches have been carried out to study adsorption mechanisms as well as the behavior of dyes with respect to the adsorbent surface [39–43]. In addition, many factors influence the rate of dye adsorption [44–46]. Consequently, the development of a mathematical model which takes into account mass transfer resistances within the adsorbent particles is necessary to predict the adsorption capacity of dye.

The objective of this study was to develop a mathematical model and simulate the organic dye of MB adsorption on modified MOF-5 ($H_6P_2W_{18}O_{62}$/MOF-5) [38]. A mathematical model was assessed based on a two-resistance model which included external mass transfer coefficient and pore diffusion coefficient that controls the mass transfer process in batch MB dye adsorption. The developed mathematical model was then used to calculate the mass transfer parameters, i.e., mass transfer coefficient and pore diffusion coefficient. Simulations with MATLAB software were then carried out to investigate the effect of various factors affecting the MB dye adsorption, namely, modification of MOF-5, temperature, initial dye concentration, and adsorbent dosage.

2 Model Development

The film-pore diffusion model proposed by Spahn and Schlünder [47] was used to model the batch MB dye adsorption on modified MOF-5 ($H_6P_2W_{18}O_{62}$/MOF-5) [38]. This model was developed using the following several assumptions: (a) the adsorbent particle has a spherical shape, (b) the mass transport of solute molecules within the pores of an adsorbent particle is only by molecular diffusion, (c) the driving force in both film and particle mass transfer is linear, and (d) pore diffusivity is independent of concentration. The amount of dye absorbed at

equilibrium (q_e)[1)], was determined by the Langmuir equation [48], as defined below:

$$q_e = \frac{q_m K_L C_e}{1 + K_L C_e} \tag{1}$$

where C_e is the equilibrium concentration of the adsorbate, q_m is the maximum adsorption capacity, and K_L is the Langmuir constant. Eqs. (2) and (3) are used in the current model to represent the kinetics of the adsorption process for spherical adsorbent particles [49]. The mass transfer at the external surface of the adsorbent particles is represented by:

$$N(t) = 4\pi R^2 k_f (C_t - C_e) \tag{2}$$

where k_f is the external mass transfer coefficient and C_t is the liquid phase concentration at time t. The mass transfer of solute through the pores is given by:

$$N = 4\pi r^2 D_p \frac{dC}{dr} \tag{3}$$

Integrating Eq. (3) for the boundary conditions C=0 to C=C_e at r=r to r=R, and rearrange it to yield:

$$N = \frac{4\pi D_p C_e}{\left(\frac{1}{r} - \frac{1}{R}\right)} \tag{4}$$

where D_p, r, and R are the pore diffusion coefficient, radius of concentration front (radius of dye concentration that penetrates the adsorbent particle), and adsorbent particle radius, respectively. The adsorption rate $N(t)$ is related to the differential mass balance over the system by equating the decrease in dye concentration in the solution with the accumulation of the adsorbate in the MOF-5 particle and the mass balance on a spherical element of adsorbate particle as given by Eq. (5) [49]:

$$N(t) = -4\pi r^2 q_e \rho \frac{dr}{dt} \tag{5}$$

where ρ is the adsorbent density. Equating Eqs. (2) and (5) and rearranging gives the following equation:

$$C_e = C + \frac{r^2 q_e \rho}{R^2 k_f} \frac{dr}{dt} \tag{6}$$

Equating Eqs. (4) and (5) and rearranging yields:

$$-r\frac{dr}{dt} = \frac{D_p C_e}{q_e \rho \left(1 - \frac{r}{R}\right)} \tag{7}$$

Substitution of Eq. (6) into Eq. (7) and rearranging the equation leads to:

$$-\frac{dr}{dt}\left[r + \frac{r^2 D_p}{R^2 k_f \left(1 - \frac{r}{R}\right)}\right] = \frac{D_p C}{q_e \rho \left(1 - \frac{r}{R}\right)} \tag{8}$$

The average dye concentration in the adsorbent particle (adsorption capacity) is defined by Eq. (9) [49]:

$$q = q_e \left[1 - \left(\frac{r}{R}\right)^3\right] \tag{9}$$

Rearranging Eq. (9) gives:

$$r = R\left[1 - \frac{q}{q_e}\right]^{\frac{1}{3}} \tag{10}$$

The following equation is obtained by differentiation of Eq. (10):

$$dr = -\frac{R}{3q_e}\left[1 - \frac{q}{q_e}\right]^{-\frac{2}{3}} dq \tag{11}$$

Substitution of Eqs. (10) and (11) into Eq. (8) and rearranging the equation yields the following form:

$$\left[1 - \frac{q}{q_e}\right]^{-\frac{2}{3}} \frac{dq}{dt}\left[\left[1 - \frac{q}{q_e}\right]^{\frac{1}{3}} dq + \frac{\left[1 - \frac{q}{q_e}\right]^{\frac{2}{3}} D_p}{R k_f \left(1 - \left[1 - \frac{q}{q_e}\right]^{\frac{1}{3}}\right)}\right] = \frac{3 D_p C}{R^2 \rho \left(1 - \left[1 - \frac{q}{q_e}\right]^{\frac{1}{3}}\right)} \tag{12}$$

To characterize the model behavior, the Biot number (Bi) expression was used and is given by Inglezakis et al. [50]:

$$Bi = \frac{k_f R}{D_p} \tag{13}$$

Substitution of Eq. (13) into Eq. (12) and rearranging the equation gives:

$$\frac{dq}{dt} = \frac{3 D_p C \left[1 - \frac{q}{q_e}\right]^{\frac{1}{3}}}{R^2 \rho \left[1 - \left(1 - \frac{1}{Bi}\right)\left(1 - \left[1 - \frac{q}{q_e}\right]^{\frac{1}{3}}\right)\right]} \tag{14}$$

The mass balance between the liquid phase concentration and the amount of adsorbate in the adsorbent is defined by Choy et al. [51]:

$$V(C_0 - C) = qW \tag{15}$$

Rearranging Eq. (15) leads to:

$$C = C_0 - \frac{qW}{V} \tag{16}$$

where C_0, W, and V are the initial liquid phase concentration, mass of adsorbent, and volume of liquid phase, respectively. Substituting Eq. (16) into Eq. (14) gives:

1) List of symbols at the end of the paper.

$$\frac{dq}{dt} = \frac{3D_p\left[C_0 - \frac{qW}{V}\right]\left[1 - \frac{q}{q_e}\right]^{\frac{1}{3}}}{R^2\rho\left[1 - \left(1 - \frac{1}{Bi}\right)\left(1 - \left[1 - \frac{q}{q_e}\right]^{\frac{1}{3}}\right)\right]} \quad (17)$$

Eq. (17) is solved by the programming language written in MATLAB R2020b software. The two unknown parameters, namely, external mass transfer coefficient (k_f) and pore diffusion coefficient (D_p), which present the best fit between experimental data and model data, were predicted by minimizing the difference between experimental and simulated the data via *fminsearch* in MATLAB. The error of experimental and simulated data was calculated by root mean squared error (*RMSE*) [52], given by the following form:

$$RMSE = \sqrt{\frac{1}{n}\sum_{i=1}^{n}\left(q_{e,exp} - q_{e,cal}\right)_i^2} \quad (18)$$

where n is the number of data per experimental data set, $q_{e,exp}$ and $q_{e,cal}$ are the adsorbed amounts obtained from the experiment and the adsorption isotherm model, respectively.

The input parameter data were taken from Liu et al. [38] and is indicated in Tab. 1. This data was used to calculate the two unknown parameters (k_f and D_p). Then, simulation with MATLAB was performed to study the effect of MOF-5 modification, temperature, initial dye concentration, and adsorbent dosage towards MB dye adsorption.

Table 1. Input parameters.

Parameters	Value
Volume of liquid phase V [L]	0.02
Mass of adsorbent W [g]	0.015
Particle density of adsorbent ρ [kg m^{-3}]	3349[a)]
Radius of adsorbent particle size R [m]	1.023×10^{-3} [a)]
Maximum adsorption capacity q_m [mg g^{-1}]	51.81[b)]
Langmuir constant K_L [L g^{-1}]	1.75[b)]

[a)] Calculated; [b)] value for a temperature of 313 K.

3 Results and Discussion

3.1 Parameter Estimation

In this current work, the film-pore diffusion model is developed based on external mass transfer coefficient (k_f) and pore diffusion coefficient (D_p) of adsorbate molecules of MB dye on modified MOF-5 by using the experimental data obtained from Liu et al. [38]. The external mass transfer coefficient is related to the external liquid film resistance whereas the internal pore diffusion coefficient represents the intraparticle diffusion resistance in the pores of adsorbents, and these two parameters are required to be estimated by using *fminsearch* via MATLAB program. These parameters were calculated by minimizing errors between model and experimental data (*RMSE*). The values of k_f and D_p that provide the best fit of model with experimental data from the adsorption of MB dye on modified MOF-5 were found to be 66.8 m s^{-1} and 2.15×10^{-7} m^{2}s^{-1}, respectively.

Different results were obtained in comparison to a previous study conducted by Choy et al. [51] on acid blue dye adsorption by using activated carbon. They found that the values for k_f and D_p were 1.56×10^{-6} m s^{-1} and 1.56×10^{-7} m^{2}s^{-1}, respectively. This is probably due to the different type of adsorbent and adsorbate used. Since k_f represents the external mass transfer coefficient, the higher value of k_f may indicate that the effect of external film diffusion is stronger in the adsorption of MB dye on modified MOF-5.

To analyze the error (*RMSE*) of the developed film-pore diffusion model, the estimated k_f and D_p values were applied to simulate batch MB dye adsorption on modified MOF-5 at initial dye concentrations of 20, 25, and 30 mg L^{-1}. Fig. 1 shows the experimental data and the simulated concentration profiles at different initial dye concentrations. It was shown that the film-pore diffusion model fits well with the experimental data for initial concentration of 20 and 25 mg L^{-1}, but for 30 mg L^{-1} the model slightly diverges with experimental data.

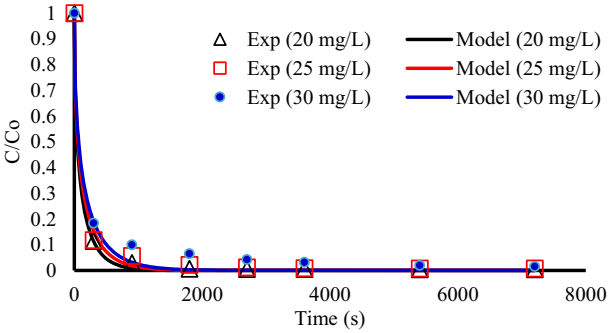

Figure 1. Concentration profile at various initial MB dye concentrations.

Tab. 2 presents the *RMSE* resulting from the simulation of batch MB dye adsorption on modified MOF-5 at different initial dye concentrations. It shows that the *RMSE* rises when the initial dye concentration increases. The initial dye concentration of 30 mg L^{-1} gives the highest value of *RMSE* followed by 25 and 20 mg L^{-1}. The higher value of *RMSE* indicates the poor correlation between experimental data and simulated data (model). However, the simulation results demonstrate that the film-pore diffusion model is able to fit the experimental data

Table 2. Calculated coefficient parameters, Biot numbers, and *RMSE* at different initial dye concentrations.

Initial conc. C_0 [mg L^{-1}]	k_f [m s^{-1}]	D_p [m^{2}s^{-1}]	Biot number Bi [–]	*RMSE* [–]
20	66.8	2.15×10^{-7}	317 670	0.0089
25	66.8	2.15×10^{-7}	317 670	0.0210
30	66.8	2.15×10^{-7}	317 670	0.0387
Average *RMSE*				0.0229

using a wide range of initial dye concentrations and the result for 30 mg L^{-1} is still acceptable.

Furthermore, the Biot number (*Bi*) measures the ratio of internal to external mass transfer resistances. A higher value of *Bi* would indicate an increase of intraparticle diffusion resistance [53]. The external mass transfer across the liquid layer occurs in mass transport process for Biot numbers less than 1, whereas for Biot numbers of more than 100, the pore diffusion dominates the mass transport mechanism in an adsorption process. If the Biot number is between 1 and 100, both mass transfer processes are important in the diffusion mechanism [51]. From the simulation result, the value of *Bi* obtained is 317 670 indicating that the internal pore diffusion is the rate-controlling step.

3.2 Effect of MOF-5 Modification

As reported by Liu et al. [38] the characteristics of pure MOF-5 and modified MOF-5 were different. The BET surface area and total pore volume of the modified MOF-5 ($H_6P_2W_{18}O_{62}$/MOF-5) were higher (395 m^2g^{-1} and 0.2986 cm^3g^{-1}, respectively) than the pure MOF-5 (92 m^2g^{-1} and 0.0729 cm^3g^{-1}, respectively). The difference in BET surface area and pore volume will change the value of density and radius of adsorbent as observed in Tab. 3. The density of the modified MOF-5 is smaller than that of pure MOF-5. The radius of modified MOF-5 is slightly bigger than of pure MOF-5. The relation between density, radius, and surface area may indicate that the modified MOF-5 has a greater accessibility to pores.

Table 3. Values of density and radius of pure MOF-5 and modified MOF-5 adsorbent.

Sample	ρ [kg m^{-3}]	R [m]
Modified MOF-5	3349	1.023×10^{-3}
MOF-5	13 717	0.639×10^{-3}

Fig. 2 presents the result of the simulation to study the effect of modification of MOF-5 in comparison to pure MOF-5. It can be seen that within 10 min the adsorption capacities of both MOF-5 and modified MOF-5 had clearly reached equilibrium condition. However, the time taken to reach the equilibrium for modified MOF-5 is shorter (approximately 5 min) than pure MOF-5. The higher adsorption capacity by particles adsorbent is attributed to greater accessibility to pores and larger surface area for bulk adsorption per unit weight [54]. Thus, it has been proven that the modification of MOF-5 by the addition of Wells-Dawson acids ($H_6P_2W_{18}O_{62}$) had a significant effect on the structure of MOF-5, greatly increasing the surface area and pore volume, which were all favorable factors for improving the adsorption capacity towards MB dye [38].

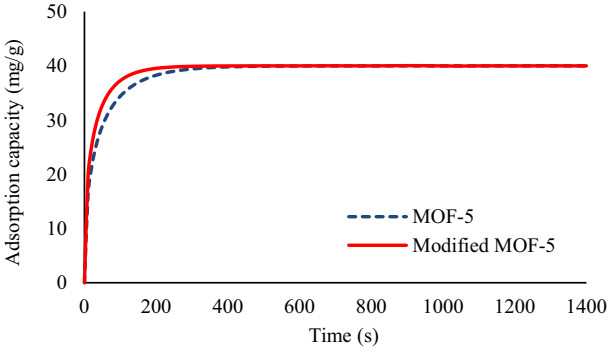

Figure 2. Comparison of MB dye adsorption capacity between pure MOF-5 and modified MOF-5 ($H_6P_2W_{18}O_{62}$/MOF-5). Conditions: W = 0.015 g, T = 313 K, V = 0.02 L, C_0 = 30 mg L^{-1}.

3.3 Effect of Initial Dye Concentration

The simulation results on the effect of initial MB dye concentration on the amount of dye adsorbed per unit mass of adsorbent (mg g^{-1}) are depicted in Fig. 3. From the simulation results, it can be concluded that the adsorption capacity of the modified MOF-5 increased with higher initial MB dye concentration. Liu et al. [38] reported that the adsorption capacity for the modified MOF-5 increased gradually from 26.75 to 52.65 mg g^{-1} with rising initial MB dye concentration. Furthermore, due to the available vacant surface area in the modified MOF-5 during the initial stage, the adsorption process could reach an equilibrium state rapidly within the first 300 s (5 min) for all the adsorbents tested at various initial MB dye concentrations. This finding indicates that the rapid removal of MB dye from aqueous solutions might be due to the complexes of particle and active species present in the modified MOF-5 adsorbent.

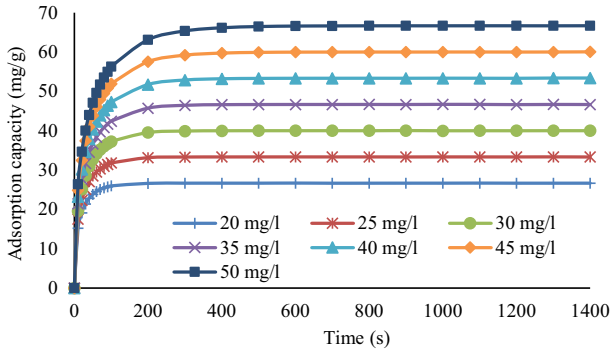

Figure 3. Effect of initial MB dye concentration on the adsorption capacity of modified MOF-5. Conditions: W = 0.015 g, T = 313 K, V = 0.02 L.

3.4 Effect of Temperature

Temperature has a significant impact on dye removal. To determine the effect of temperature on MB dye adsorption on modified MOF-5, the simulation was run at temperatures of 293, 303, and 313 K by taking into account the values of maximum adsorption capacity (q_m) and Langmuir constant (K_L) [38]. These values are listed in Tab. 4, and it is clear that the values of q_m and K_L increased with temperature. Using these values in the developed model, the simulation results at various temperatures are illustrated in Fig. 4.

Table 4. Langmuir parameters for the adsorption of MB dye onto modified MOF-5 at various temperatures [38].

Temp. [K]	q_m [mg g^{-1}]	K_L [L g^{-1}]
293	51.81	1.75
303	52.83	2.78
313	54.79	5.27

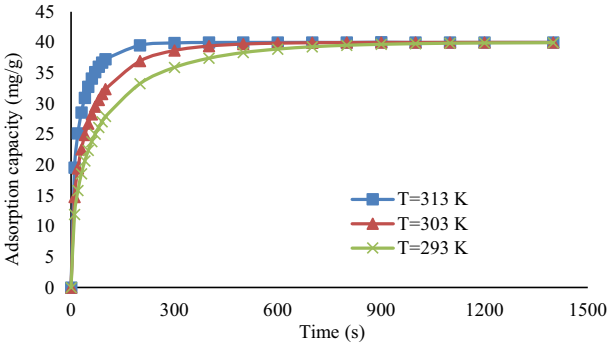

Figure 4. Effect of temperature on the adsorption capacity of modified MOF-5. Conditions: W = 0.015 g, V = 0.02 L, C_0 = 30 mg L^{-1}.

The results showed that the highest adsorption capacity was at 313 K, while at 293 K the adsorption capacity was the lowest. The increment of adsorption capacity of MB dye with temperature was due to the enhanced mobility of dye molecules at higher temperature. Furthermore, this phenomenon occurs because the viscosity of the solution decreases at high temperatures, resulting in an increased rate of diffusion of adsorbate molecules between the outer boundary layer and the inner pores on the adsorbent [55]. In addition, this data implies that MB dye adsorption onto modified MOF-5 was an endothermic process that was favored at high temperatures [56].

3.5 Effect of Adsorbent Dosage

The dosage of the adsorbent used has a significant impact on adsorption performance. The effect of adsorbent dosage on the adsorption of MB dye was evaluated at different amounts of modified MOF-5 from 0.015 g to 0.045 g, and the simulation results are presented in Fig. 5. It was demonstrated that the adsorption capacity decreases with increasing the amount of modified MOF-5, possibly due to the smaller surface area and the lack of binding sites at higher dosages. According to Khodaie et al. [57], this phenomenon can also be explained by the increase in mass of adsorbent at constant MB dye concentration and volume which will lead to a large excess of active sites through the adsorption process. Another reason could be due to the agglomeration of smaller particles during the interaction/adsorption process at high adsorbent dosage [58, 59].

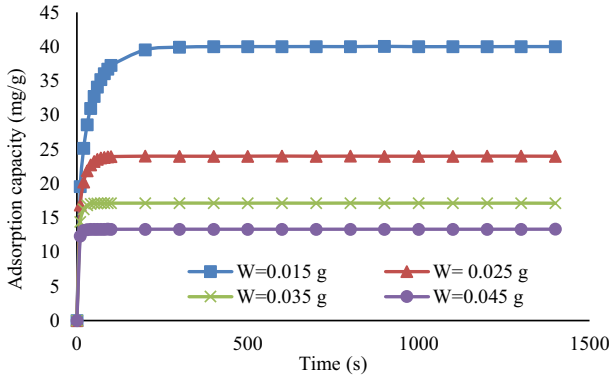

Figure 5. Effect of adsorbent dosage on the adsorption capacity of modified MOF-5. Conditions: T = 313 K, V = 0.02 L, C_0 = 30 mg L^{-1}.

4 Conclusions

A mathematical model based on a film-pore diffusion model has been developed to simulate the adsorption of the organic dye methylene blue on a modified MOF-5 ($H_6P_2W_{18}O_{62}$/MOF-5) adsorbent. The two parameters, namely, external mass transfer coefficient (k_f) and pore diffusion coefficient (D_p), have been estimated by using MATLAB software through minimizing *RMSE* values. The values of k_f and D_p that provided the best fit of the model with experimental data from the adsorption of MB dye on modified MOF-5 were estimated to be 66.8 m s^{-1} and 2.15×10^{-7} m^{2}s^{-1}, respectively.

By using the programming language written in MATLAB software, the model has been effectively applied to simulate the influence of MOF-5 modification, initial dye concentration, temperature, and adsorbent dosage. Based on the model's simulation, it was concluded that the adsorption of MB dye was higher for modified MOF-5, lower initial MB dye concentration, higher temperature, and lower adsorbent dosage.

Data Availability Statement

The data that support the findings of this study are available from the corresponding author upon reasonable request.

Acknowledgment

The authors gratefully acknowledge the support from the Ministry of Higher Education Malaysia for Fundamental Research Grant Scheme (FRGS) with Project Code FRGS/1/2019/TK02/USM/02/2 and the Universiti Sains Malaysia.

The authors have declared no conflict of interest.

Symbols used

Bi	[–]	Biot number
C	[mg L^{-1}]	concentration of liquid phase

C_0	[mg L^{-1}]	initial concentration of liquid phase
C_e	[mg L^{-1}]	equilibrium concentration of liquid phase
C_t	[mg L^{-1}]	liquid phase concentration at time t
D_p	[m^{2}s^{-1}]	pore diffusion coefficient
k_f	[m s^{-1}]	external mass transfer coefficient
K_L	[L g^{-1}]	Langmuir constant
n	[–]	number of data
N	[m s^{-1}]	adsorption rate
$N(t)$	[m s^{-1}]	adsorption rate at time t
q	[m g^{-1}]	adsorption capacity
q_e	[m g^{-1}]	amount of dye absorbed at equilibrium
q_m	[m g^{-1}]	maximum adsorption capacity
r	[m]	radius of concentration front
R	[m]	adsorbent particle radius
$RMSE$	[–]	root mean squared error
T	[K]	temperature
V	[m^3]	volume of liquid phase
W	[g]	mass of adsorbent

Greek letter

ρ	[kg m^{-3}]	adsorbent density

Subscripts

cal	calculated
exp	experimental
i	ith fraction

Abbreviations

AC	activated carbon
CAGR	compound annual growth rate
MB	methylene blue
MOF	metal-organic framework
MOF-5	metal-organic framework-5
RhB	rhodamine B

References

[1] D. A. Yaseen, M. Scholz, *Int. J. Environ. Sci. Technol.* **2019**, *16*, 1193–1226. DOI: https://doi.org/10.1007/s13762-018-2130-z

[2] H. B. Slama, A. C. Bouket, Z. Pourhassan, F. N. Alenezi, A. Silini, H. Cherif-Silini, T. Oszako, L. Luptakova, P. Goliń-ska, L. Belbahri, *Appl. Sci.* **2021**, *11*, 6255. DOI: https://doi.org/10.3390/app11146255

[3] Z. Xinhua, Analysis of China's Dye Production, Consumption and Development Prospects in 2021, *China Text.* **2021**. http://cntex2006.com/NewsView.asp?SortID=10&ID=1515

[4] *Dyes & Pigments Market Size, Share & Trends Analysis Report By Product (Dyes, Pigments), By Application, By Regions, And Segment Forecasts, 2022–2030*, Market Analysis Report, Grand View Research, Inc., San Francisco, CA **2021**. www.grandviewresearch.com/industry-analysis/dyes-and-pigments-market

[5] V. K. Gupta, Suhas, *J. Environ. Manage.* **2009**, *90*, 2313–2342. DOI: https://doi.org/10.1016/j.jenvman.2008.11.017

[6] E. Routoula, S. V. Patwardhan, *Environ. Sci. Technol.* **2020**, *54 (2)*, 647–664. DOI: https://doi.org/10.1021/acs.est.9b03737

[7] K. G. Pavithra, P. S. Kumar, V. Jaikumar, P. S. Rajan, *J. Ind. Eng. Chem.* **2019**, *75*, 1–19. DOI: https://doi.org/10.1016/j.jiec.2019.02.011

[8] P. S. Thue, A. C. Sophia, E. C. Lima, A. G. N. Wamba, W. S. de Alencar, G. S. dos Reis, F. S. Rodembusch, S. L. P. Dias, *J. Cleaner Prod.* **2018**, *171*, 30–44. DOI: https://doi.org/10.1016/j.jclepro.2017.09.278

[9] Y. Zhang, J. Zheng, J. Nan, C. Gai, Q. Shao, V. Murugadoss, S. Maganti, N. Naik, H. Algadi, M. Huang, B. B. Xu, Z. Guo, *Particuology* **2023**, *74*, 141–155. DOI: https://doi.org/10.1016/j.partic.2022.05.010

[10] P. Jadhav, S. Shinde, S. S. Suryawanshi, S. B. Teli, P. S. Patil, A. A. Ramteke, N. G. Hiremath, N. R. Prasad, *Eng. Sci.* **2020**, *12*, 79–94. DOI: https://doi.org/10.30919/es8d1138

[11] S. Fallah, H. R. Mamaghani, R. Yegani, N. Hajinajaf, B. Pour-abbas, *Adv. Compos. Hybrid Mater.* **2020**, *3*, 187–193. DOI: https://doi.org/10.1007/s42114-020-00146-4

[12] Z. Sun, Y. Zhang, S. Guo, J. Shi, C. Shi, K. Qu, H. Qi, Z. Huang, V. Murugadoss, M. Huang, Z. Guo, *Adv. Compos. Hybrid Mater.* **2022**, *5*, 1566–1581. DOI: https://doi.org/10.1007/s42114-022-00477-4

[13] R. Kumar, A. Umar, R. Kumar, M. S. Chauhan, G. Kumar, S. Chauhan, *Eng. Sci.* **2021**, *16*, 288–300. DOI: https://doi.org/10.30919/es8d548

[14] K. Xie, S. Wei, A. Alhadhrami, J. Liu, P. Zhang, A. Y. Elnag-gar, F. Zhang, M. H. H. Mahmoud, V. Murugadoss, S. M. El-Bahy, F. Wang, C. Li, G. Li, *Adv. Compos. Hybrid Mater.* **2022**, *5*, 1423–1432. DOI: https://doi.org/10.1007/s42114-022-00520-4

[15] R. B. Rajput, S. N. Jamble, R. B. Kale, *Eng. Sci.* **2021**, *17*, 176–184. DOI: https://doi.org/10.30919/es8d534

[16] Y. Si, J. Li, B. Cui, D. Tang, L. Yang, V. Murugadoss, S. Mag-anti, M. Huang, Z. Guo, *Adv. Compos. Hybrid Mater.* **2022**, *5*, 1180–1195. DOI: https://doi.org/10.1007/s42114-022-00446-x

[17] M. Cheng, C. Yao, Y. Su, J. Liu, L. Xu, J. Bu, H. Wang, S. Hou, *Eng. Sci.* **2022**, *18*, 299–307. DOI: https://doi.org/10.30919/es8d603

[18] B. S. Kaith, J. Sharma, Sukriti, S. Sethi, T. Kaur, U. Shanker, V. Jassal, *J. Chin. Adv. Mater. Soc.* **2016**, *4*, 249–268. DOI: https://doi.org/10.1080/22243682.2016.1214923

[19] C. Arora, S. Soni, S. Sahu, J. Mittal, P. Kumar, P. K. Bajpai, *J. Mol. Liq.* **2019**, *284*, 343–352. DOI: https://doi.org/10.1016/j.molliq.2019.04.012

[20] A. H. Hashem, E. Saied, M. S. Hasanin, *Sustainable Chem. Pharm.* **2020**, *18*, 100333. DOI: https://doi.org/10.1016/j.scp.2020.100333

[21] Y. Zhou, J. Lu, Y. Zhou, Y. Liu, *Environ. Pollut.* **2019**, *252*, 352–365. DOI: https://doi.org/10.1016/j.envpol.2019.05.072

[22] J. El-Gaayda, F. E. Titchou, R. Oukhrib, P.-S. Yap, T. Liu, M. Hamdani, R. A. Akbour, *J. Environ. Chem. Eng.* **2021**, *9 (5)*, 106060. DOI: https://doi.org/10.1016/j.jece.2021.106060

[23] L. Liu, Z. Chen, J. Zhang, D. Shan, Y. Wu, L. Bai, B. Wang, *J. Water Process Eng.* **2021**, *42*, 102122. DOI: https://doi.org/10.1016/j.jwpe.2021.102122

[24] A. Haji, M. Naebe, *J. Cleaner Prod.* **2020**, *265*, 121866. DOI: https://doi.org/10.1016/j.jclepro.2020.121866

[25] G. K. Weldegebrieal, *Inorg. Chem. Commun.* **2020**, *120*, 108140. DOI: https://doi.org/10.1016/j.inoche.2020.108140
[26] C. Jing, Y. Zhang, J. Zheng, S. Ge, J. Lin, D. Pan, N. Naik, Z. Guo, *Particuology* **2022**, *69*, 111–122. DOI: https://doi.org/10.1016/j.partic.2021.11.013
[27] R. Nandanwar, J. Bamne, N. Singh, K. Taiwade, V. Chandel, P. K. Sharma, P. Singh, A. Umar, F. Z. Haque, *ES Mater. Manuf.* **2022**, *16*, 78–88. DOI: https://doi.org/10.30919/esmm5f628
[28] N. Singh, S. Jana, G. P. Singh, R. K. Dey, *Adv. Compos. Hybrid Mater.* **2020**, *3*, 127–140. DOI: https://doi.org/10.1007/s42114-020-00140-w
[29] R. V. Kandisa, K. V. N. Saibaba, K. B. Shaik, R. Gopinath, *J. Biorem. Biodegrad.* **2016**, *7*, 371. DOI: https://doi.org/10.4172/2155-6199.1000371
[30] P. P. Bag, G. P. Singh, S. Singha, G. Roymahapatra, *Eng. Sci.* **2021**, *13*, 1–10. DOI: https://doi.org/10.30919/es8d1166
[31] W. Nong, X. Liu, Q. Wang, J. Wu, Y. Guan, *ES Food Agrofor.* **2020**, *1*, 11–40. DOI: https://doi.org/10.30919/esfaf0001
[32] Y. Wang, Y. Liu, C. Wang, H. Liu, J. Zhang, J. Lin, J. Fan, T. Ding, J. E. Ryu, Z. Guo, *Eng. Sci.* **2020**, *9*, 50–59. DOI: https://doi.org/10.30919/es8d903
[33] K. Qu, Z. Sun, C. Shi, W. Wang, L. Xiao, J. Tian, Z. Huang, Z. Guo, *Adv. Compos. Hybrid Mater.* **2021**, *4*, 670–683. DOI: https://doi.org/10.1007/s42114-021-00293-2
[34] S. ur Rehman, R. Ahmed, K. Ma, S. Xu, T. Tao, M. A. Aslam, M. Amir, J. Wang, *Eng. Sci.* **2021**, *13*, 71–78. DOI: https://doi.org/10.30919/es8d1263
[35] W. Cheng, Y. Wang, S. Ge, X. Ding, Z. Cui, Q. Shao, *Adv. Compos. Hybrid Mater.* **2021**, *4*, 150–161. DOI: https://doi.org/10.1007/s42114-020-00199-5
[36] S. Jawahery, C. M. Simon, E. Braun, M. Witman, D. Tiana, B. Vlaisavljevich, B. Smit, *Nat. Commun.* **2017**, *8*, 13945. DOI: https://doi.org/10.1038/ncomms13945
[37] S. Bennabi, M. Belbachir, *J. Mater. Environ. Sci.* **2017**, *8*, 4391–4398. DOI: https://doi.org/10.26872/jmes.2017.8.12.463
[38] X. Liu, W. Gong, J. Luo, C. Zou, Y. Yang, S. Yang, *Appl. Surf. Sci.* **2016**, *362*, 517–524. DOI: https://doi.org/10.1016/j.apsusc.2015.11.151
[39] G. Aggrwal, S. Salunke-Gawali, S. P. Gejji, M. Nikalje, D. Chakravarty, P. L. Verma, P. Gosavi-Mirkute, S. Harihar, M. Jadhav, V. G. Puranik, *Eng. Sci.* **2021**, *14*, 78–93. DOI: https://doi.org/10.30919/es8d427
[40] B. K. Rana, J. Dinda, P. K. Mahapatra, D. Chopra, V. Bertolasi, K. M. Bairagi, S. K. Nayak, H. S. Das, S. Giri, G. Roymahapatra, *Eng. Sci.* **2022**, *17*, 204–215. DOI: https://doi.org/10.30919/es8d623
[41] G. Roymahapatra, M. K. Dash, S. Sinha, G. C. De, Z. Guo, *Eng. Sci.* **2022**, *19*, 114–124. DOI: https://doi.org/10.30919/es8d671
[42] F. Hu, L. Wang, Y. Liu, M. M. Hessien, I. H. El Azab, S. Jing, A. Y. Elnaggar, S. M. El-Bahy, M. Huang, R. Zhang, *Adv. Compos. Hybrid Mater.* **2022**, *5*, 1307–1318. DOI: https://doi.org/10.1007/s42114-022-00506-2
[43] S. U. Jan, A. Ahmad, A. A. Khan, S. Melhi, I. Ahmad, G. Sun, C. M. Chen, R. Ahmad, *Environ. Sci. Pollut. Res.* **2021**, *28*, 10234–10247. DOI: https://doi.org/10.1007/s11356-020-11344-4
[44] M. Mobarak, A. Q. Selim, E. A. Mohamed, M. K. Seliem, *J. Cleaner Prod.* **2018**, *192*, 712–721. DOI: https://doi.org/10.1016/j.jclepro.2018.05.044
[45] I. Dahlan, K. C. Kit, *Int. J. Environ. Technol. Manage.* **2019**, *22 (1)*, 40–55. DOI: https://doi.org/10.1504/IJETM.2019.101385
[46] T. Krasnova, N. Golubeva, Y. Skolubovich, D. Volkov, N. Gora, *IOP Conf. Ser.: Mater. Sci. Eng.* **2020**, *953*, 012019. DOI: https://doi.org/10.1088/1757-899X/953/1/012019
[47] H. Spahn, E. U. Schlünder, *Chem. Eng. Sci.* **1975**, *30 (5–6)*, 529–537. DOI: https://doi.org/10.1016/0009-2509(75)80023-6
[48] E. C. Lima, M. A. Adebayo, F. M. Machado, in *Carbon Nanomaterials as Adsorbents for Environmental and Biological Applications* (Eds: C. P. Bergmann, F. M. Machado), Springer, Cham, Switzerland **2015**, Ch. 3. DOI: https://doi.org/10.1007/978-3-319-18875-1_3
[49] P. R. Jena, S. De, J. K. Basu, *Chem. Eng. J.* **2003**, *95 (1–3)*, 143–154. DOI: https://doi.org/10.1016/S1385-8947(03)00097-4
[50] V. J. Inglezakis, M. Balsamo, F. Montagnaro, *Ind. Eng. Chem. Res.* **2020**, *59*, 22007–22016. DOI: https://doi.org/10.1021/acs.iecr.0c05032
[51] K. K. H. Choy, J. F. Porter, G. McKay, *Chem. Eng. Sci.* **2004**, *59*, 501–512. DOI: https://doi.org/10.1016/j.ces.2003.10.012
[52] A. Terdputtakun, O. Arqueropanyo, P. Sooksamiti, S. Janhom, W. Naksata, *Environ. Earth Sci.* **2017**, *76*, 777. DOI: https://doi.org/10.1007/s12665-017-7110-y
[53] S. Y. Quek, B. Al-Duri, *Chem. Eng. Process.* **2007**, *46 (5)*, 477–485. DOI: https://doi.org/10.1016/j.cep.2006.06.019
[54] S. Senthilkumaar, P. R. Varadarajan, K. Porkodi, C. V. Subbhuraam, *J. Colloid Interface Sci.* **2005**, *284 (1)*, 78–82. DOI: https://doi.org/10.1016/j.jcis.2004.09.027
[55] S. Karaca, A. Gürses, M. Açikyildiz, M. Ejder (Korucu), *Microporous Mesoporous Mater.* **2008**, *115 (3)*, 376–382. DOI: https://doi.org/10.1016/j.micromeso.2008.02.008
[56] Y. Kuang, X. Zhang, S. Zhou, *Water* **2020**, *12 (2)*, 587. DOI: https://doi.org/10.3390/w12020587
[57] M. Khodaie, N. Ghasemi, B. Moradi, M. Rahimi, *J. Chem.* **2013**, *2013*, 383985. DOI: https://doi.org/10.1155/2013/383985
[58] S. Shakoor, A. Nasar, *J. Taiwan Inst. Chem. Eng.* **2016**, *66*, 154–163. DOI: https://doi.org/10.1016/j.jtice.2016.06.009
[59] C. Li, Y. Dong, D. Wu, L. Peng, H. Kong, *Appl. Clay Sci.* **2011**, *52 (4)*, 353–357. DOI: https://doi.org/10.1016/j.clay.2011.03.015

Research Article: A mathematical model based on a film-pore diffusion model has been developed to simulate the adsorption of the organic dye methylene blue on a modified metal-organic framework-5 ($H_6P_2W_{18}O_{62}$/MOF-5) adsorbent. The model has been effectively applied to simulate the influence of MOF-5 modification, initial dye concentration, temperature, and adsorbent dosage.

Modeling of Batch Organic Dye Adsorption Using Modified Metal-Organic Framework-5

Irvan Dahlan*,
Wan Hamizan Wan Mazlan, Andi Mulkan, Haider M. Zwain, Siti Roshayu Hassan, Hamidi Abdul Aziz, Harahsheh Yazeed Ahmad Hasan, Ivar Zekker

Chem. Eng. Technol. **2022**, *45 (XX)*, XXX … XXX

DOI: 10.1002/ceat.202200042